

Magnetic resonance in the pyrochlore antiferromagnet $\text{Gd}_2\text{Ti}_2\text{O}_7$

S. S. Sosin, A. I. Smirnov, and L. A. Prozorova

P. L. Kapitza Institute for Physical Problems RAS, 119334 Moscow, Russia

G. Balakrishnan

Department of Physics, University of Warwick, Coventry CV4 7AL, United Kingdom

M. E. Zhitomirsky

Commissariat à l'Energie Atomique, DSM/DRFMC/SPSMS, 38054 Grenoble, France

(Received 24 March 2006; revised manuscript received 13 April 2006; published 2 June 2006)

An electron spin resonance study of frustrated pyrochlore $\text{Gd}_2\text{Ti}_2\text{O}_7$ is performed in a wide frequency band for a temperature range 0.4–30 K, which covers paramagnetic and magnetically ordered phases. The paramagnetic resonance reveals a spectroscopic g factor of about 2.0 and a temperature-dependent linewidth. In ordered phases magnetic resonance spectra are distinctive for a nonplanar cubic (or tetrahedral) antiferromagnet with an isotropic susceptibility. In the high-field-saturated phase, weakly dispersive soft modes are observed and their field evolution is traced.

DOI: [10.1103/PhysRevB.73.212402](https://doi.org/10.1103/PhysRevB.73.212402)

PACS number(s): 76.50.+g, 75.50.Ee, 75.30.-m

Frustrated antiferromagnets are among the most interesting strongly correlated magnetic systems. The geometry of a crystal lattice in these compounds does not allow the energy of all paired exchange bonds to be minimized simultaneously. In the case of pyrochlore the geometry of corner-sharing tetrahedra frustration leads to a macroscopic number of classical ground states. Strong fluctuations between degenerate ground states preclude any conventional type of magnetic ordering.¹ Eventually, degeneracy is removed by weak residual interactions (dipolar, next-nearest-neighbor exchange, relativistic anisotropy) or by short-wavelength fluctuations (order-by-disorder effect). Such a degeneracy lifting occurs with the two major consequences: (i) if a long-range ordering does occur in such a system, it develops at temperatures much lower than in a usual nonfrustrated antiferromagnet with a similar magnitude of the exchange integral, and (ii) a delicate balance between a number of weak interactions yields a large variety of possible outcomes so that similar compounds can reveal drastically different magnetic properties.

A nice example of the above principles is provided by two pyrochlore compounds $\text{Gd}_2\text{Ti}_2\text{O}_7$ and $\text{Gd}_2\text{Sn}_2\text{O}_7$. Magnetic Gd^{3+} ions with semiclassical spins $S=7/2$ have zero orbital momentum and, consequently, reduced crystal field effects compared to other rare-earth compounds. Both gadolinium pyrochlores have complicated phase diagrams. Magnetic ordering in $\text{Gd}_2\text{Ti}_2\text{O}_7$ takes place at $T_{c1} \approx 1$ K followed by a second transition at $T_{c2} \approx 0.75$ K.^{2,3} At $T < T_{c2}$ two field-induced transitions are observed under a magnetic field at $H_{c1} \approx 30$ kOe and $H_{c2} \approx 60$ –70 kOe (above H_{c2} the magnetic moment is close to saturation). A single first-order phase transition occurs in $\text{Gd}_2\text{Sn}_2\text{O}_7$ at $T_c \approx 1$ K.⁴ A recent neutron diffraction study has identified the low-temperature phase of $\text{Gd}_2\text{Ti}_2\text{O}_7$ to be a multi- k structure described by four wave vectors of the type $\mathbf{k} = (\frac{1}{2} \frac{1}{2} \frac{1}{2})$ with partial disorder of one-fourth of magnetic moments.⁵ This type of structure can be stabilized due to dipolar interaction in combination with a next-nearest-neighbor superexchange.^{6–8} Another possibility is provided by strong fluctuations choosing the state with

$\mathbf{k}=(000)$,^{7,9} which was recently observed in $\text{Gd}_2\text{Sn}_2\text{O}_7$.

An important consequence of a macroscopic number of nearly degenerate states in a geometrically frustrated magnet is that its excitation spectrum contains soft, almost dispersionless modes in the whole Brillouin zone. Neutron experiments¹⁰ in the frustrated spinel compound ZnCr_2O_4 indicate such modes to exist above the ordering temperature. Almost degenerate modes lead to a large residual entropy and an enhanced magnetocaloric effect,¹¹ which has been measured in $\text{Gd}_2\text{Ti}_2\text{O}_7$ and a garnet $\text{Gd}_3\text{Ga}_5\text{O}_{12}$.¹² The dynamics of these modes below ordering cannot be treated as a conventional antiferromagnetic resonance. Uniform oscillations of spins in crystals near an equilibrium state (fixed by weak forces) are accompanied by an absence of spin stiffness usually provided by the strongest exchange interaction. It is not obvious *a priori* whether such modes should be resonance spin oscillations or a kind of relaxation movement. Since inelastic neutron scattering experiments are hindered by a large absorption cross section of gadolinium ions, electron spin resonance (ESR) appears to be the most convenient technique to probe the low-energy excitation spectra in $\text{Gd}_2\text{Ti}_2\text{O}_7$ and $\text{Gd}_2\text{Sn}_2\text{O}_7$.

In the present work we study a single crystal of $\text{Gd}_2\text{Ti}_2\text{O}_7$ in wide frequency and field ranges at temperatures both above and below $T_{c1,2}$. The magnetic resonance signals are observed and analyzed in the paramagnetic and in all four ordered phases. At the lowest experimental temperature 0.42 K two resonance branches with different energy gaps are observed at fields below H_{c1} . In the intermediate range $H_{c1} < H < H_{c2}$ the field-dependent gap of the magnon branch, softening in the vicinity of the spin-flip transition H_{c2} , is found. In the spin-saturated phase three weak and narrow resonance modes are detected, two of them corresponding to “soft modes” with weak dispersion, in agreement with spin-wave calculations.

A single crystal of $\text{Gd}_2\text{Ti}_2\text{O}_7$ has been grown by a floating-zone technique.¹³ We studied two small samples cut in a form of thin square plates of approximately $1 \times 1 \times 0.1$ mm³ in size (0.5–0.6 mg by mass) with their [111]

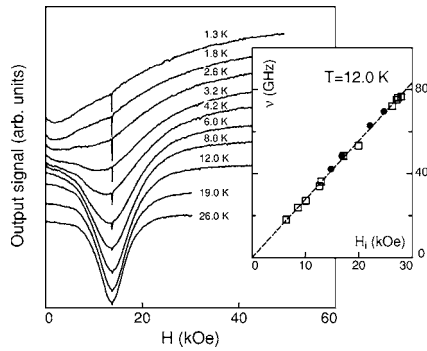


FIG. 1. The field dependence of the resonance absorption in $\text{Gd}_2\text{Ti}_2\text{O}_7$ at $\nu=36.2$ GHz ($H \perp [111]$ axis) for various temperatures above T_{N1} . The inset shows the frequency-field diagram for $T=12$ K (solid and open circles correspond to $H \perp [111]$ and $H \parallel [111]$, respectively); the dashed line is a paramagnetic resonance with $g=2$.

axes oriented parallel and perpendicular to the sample plane. The resonance measurements are performed in a set of transmission-type spectrometers with different resonators covering the frequency range 20–100 GHz. An external magnetic field up to 120 kOe created by a cryomagnet was always applied in a sample plane so that no correction for the demagnetization factor is required.

Measurements in the temperature range 1.2–30 K are carried out in a ^4He cryostat. The corresponding field scans taken at a frequency 36.2 GHz for various temperatures are shown in Fig. 1. At high temperatures $T \gg \theta_{CW} \approx 10$ K a single resonance line with linewidth $\Delta H \sim 3$ kOe is observed in all magnetic field orientations. It has a linear frequency-field dependence with an isotropic g factor 2.0 (see inset in Fig. 1). On decreasing the temperature below 10 K the resonance line starts to broaden and decrease in amplitude. In the vicinity of the upper ordering transition T_{c1} the line transforms into a wide nonresonant band of absorption having its maximum at zero magnetic field. The splitting of the resonance line at high frequencies previously reported in Ref. 14 and attributed to the strong anisotropic effects has been also observed in our experiment. We have, however, found that such a splitting exists only for large samples and is easily eliminated by decreasing the size of the plate. This effect should therefore be attributed to the electrodynamic resonances in the dielectric sample with the field- and temperature-dependent magnetic susceptibility. A detailed analysis of the high-temperature resonance properties of $\text{Gd}_2\text{Ti}_2\text{O}_7$ and $\text{Gd}_2\text{Sn}_2\text{O}_7$ will be published elsewhere.

The low-temperature ESR spectra have been obtained in a ^3He cryostat equipped with a sorb pump enabling it to cool down to approximately 0.4 K. The resonance absorption spectra taken at $T=0.42$ K in the whole frequency range are presented in Fig. 2 for two principal orientations of the external field ($H \parallel [111]$ and $H \perp [111]$ left and right panels, respectively). Among a number of resonance lines observed below H_{c1} in both orientations one can trace absorptions belonging to two different gapped branches, one of them decreasing (line A) and the other one increasing (line B) in field (shown by the dashed lines, which are guides to eye in the Fig. 2). Other resonances are difficult to trace on changing

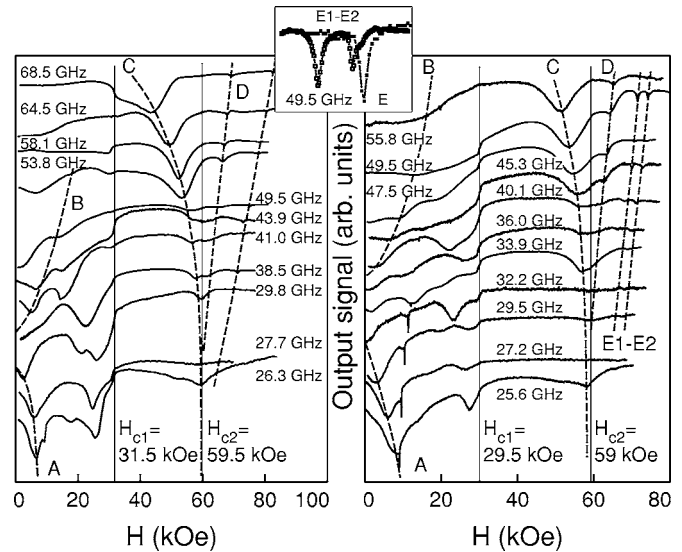


FIG. 2. The absorption spectra recorded at $T=0.42$ K at different frequencies (increasing bottom up) for $H \parallel [111]$ (left panel) and $H \perp [111]$ (right panel). Dashed lines are guides to the eye to trace the frequency evolution of the same resonance modes. Vertical solid lines mark the points of the phase transitions H_{c1} and H_{c2} . The inset expands the weak-resonance lines E and $E1-E2$ taken at the same frequency in both field orientations.

the frequency, but all of them soften or disappear in the vicinity of H_{c1} . This transition is clearly observed in both field orientations by sharp jumps at the absorption lines in both the forward and backward field sweeps without hysteresis. Just above the transition a new resonance line appears at a frequency of about 70 GHz (line C). It gradually drops on increasing the magnetic field, practically independent of its orientation, and almost softens at the second transition H_{c2} . This transition is accompanied by the appearance of two additional weak-resonance modes (lines D and E) for $H \parallel [111]$, both increasing in field. In a perpendicular field orientation line E remains unchanged while line E is split into two components (expanded in the inset in Fig. 2).

All resonance lines have a strong temperature dependence. On heating they broaden and shift (see Fig. 3) and finally disappear while the background absorption line acquires the shape observed in the preliminary high-temperature experiment. One should mention that this nonresonant low-field background also survives at temperatures below ordering.

A convenient approach to describe the low-field resonance properties of magnetically ordered systems is macroscopic hydrodynamic theory,¹⁵ which is applicable if an exchange interaction plays the principal role in magnetic ordering. Such an assumption might be incorrect for $\text{Gd}_2\text{Ti}_2\text{O}_7$, a system with a considerable single-ion anisotropy¹⁶ and ordering driven by weak interactions. We shall, however, use such a theory in an attempt to obtain a qualitative description of the experimental data. A nonplanar exchange structure can be described by three orthogonal unit vectors \mathbf{I}_n .¹⁵ For the $4k$ structure found in neutron experiments⁵ the antiferromagnetic vectors \mathbf{I}_n transform according to the three-dimensional irreducible representation

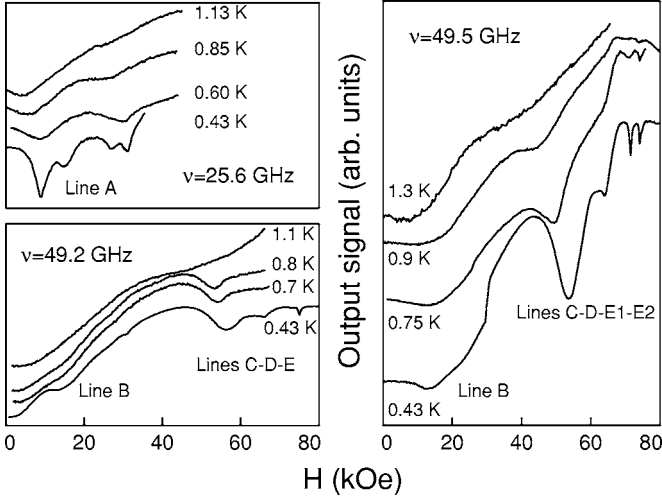


FIG. 3. The temperature evolution of the absorption lines at given frequencies for $H \parallel [111]$ (left panel) and $H \perp [111]$ (right panel).

F_1 of the tetrahedral group T_d .¹⁷ The energy of magnetic anisotropy is obtained by constructing various invariants from the components l_n^α . In the lowest order the anisotropy is expressed as

$$E_a = \lambda_1(l_{1x}^2 + l_{2y}^2 + l_{3z}^2) + \lambda_2(l_{1y}l_{2x} + l_{1z}l_{3x} + l_{2z}l_{3y}) + \lambda_3(l_{1x}l_{2y} + l_{2y}l_{3z} + l_{3z}l_{1x}), \quad (1)$$

where λ_n are phenomenological parameters. Expression (1) has five extrema; each can correspond to an equilibrium orientation of \mathbf{l}_n at some values of λ_n . Three of these states preserve the original cubic symmetry, in which case the spectrum of uniform oscillations consists of three degenerate eigenmodes, while experimentally we observe at least two different resonance branches at $H=0$. Among the two non-symmetric states, the most probable one is obtained by rotating the triad $\mathbf{l}_1=\mathbf{x}$, $\mathbf{l}_2=\mathbf{y}$, $\mathbf{l}_3=\mathbf{z}$ by an angle $\varphi = \arccos[-(2\lambda_1 - \lambda_2 + 2\lambda_3)/[4(\lambda_1 + \lambda_2 + \lambda_3)]]$ about the $[111]$ direction.

The kinetic energy of small homogeneous oscillations of the exchange structure in weak magnetic field $H \ll H_{c2}$ is determined by the susceptibility tensor,¹⁵ which has an isotropic form for this type of magnetic structure. (Magnetization measurements at $T=0.3$ K (Ref. 18) confirm that the values of χ are equal for $H \parallel [111]$ and $H \parallel [110]$.) The kinetic energy is written, therefore, as

$$K = \frac{\chi}{2} \left(\frac{\Omega}{\gamma} + H \right)^2, \quad (2)$$

where Ω is an angular velocity and $\gamma = g\mu_B/\hbar$ is a gyromagnetic ratio. Performing standard Lagrangian dynamics calculations with $\mathcal{L} = K - E_a$ one obtains the following equation for the resonance frequencies:

$$(\nu^2 - \Delta_1^2)(\nu^2 - \Delta_2^2) - \tilde{\gamma}^2 \nu^2 (\nu^2 H^2 - \Delta_1^2 H_{\parallel}^2 - \Delta_2^2 H_{\perp}^2) = 0, \quad (3)$$

where $\Delta_{1,2}$ are the gap values (a certain combination of λ_n and χ which can be treated as fitting parameters) and H_{\parallel} and

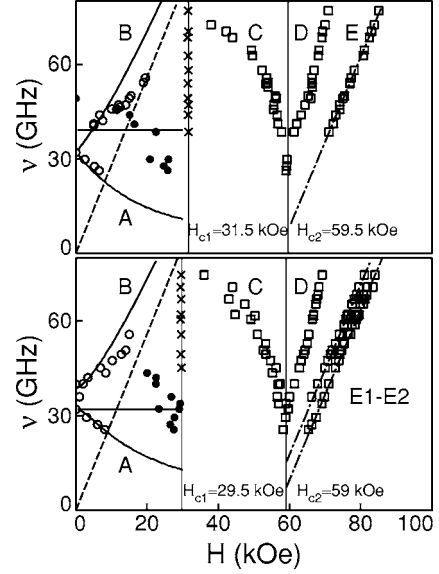


FIG. 4. Frequency field diagram of the resonance spectrum in $\text{Gd}_2\text{Ti}_2\text{O}_7$ at $T=0.42$ K for $H \parallel [111]$ (upper panel) and $H \perp [111]$ (lower panel); (\circ) low-field lines, (\square) high-field lines, (\bullet) unidentified resonances, (\times) H_{c1} transitions. Solid lines represent the low-field theoretical calculations with the parameters $\Delta_1=39$ GHz, the $\Delta_2=32$ GHz. The dashed line is a paramagnetic resonance with $g=2.0$, and dash-dotted lines are linear fits as described in the text. Phase transitions at $H=H_{c1,2}$ are pointed by vertical lines as in Fig. 2.

H_{\perp} are field components with respect to the $[111]$ axis, $\tilde{\gamma} = \gamma/2\pi$.

The calculated field dependences of all three branches for both regular field orientations are shown in Fig. 4 by solid lines with $\Delta_1=39$ GHz and $\Delta_2=32$ GHz. One can see that the description of the spectrum in the range of theory application (namely, of the low-field lines A and B) is satisfactory. However, one should mention that this theory predicts all low-lying excitations to have finite gaps, which excludes the experimentally observed power-law dependence of the specific heat down to 0.2 K.¹⁹ It also fails to explain the broad background absorption observed in an ordered phase which might reflect the non-frozen-spin behavior at low temperatures. Consequently, an “exchange softness” of the magnetic structure in $\text{Gd}_2\text{Ti}_2\text{O}_7$ remains essential down to temperatures $T \ll T_c$ and requires new theoretical approaches for a final description of the spin dynamics.

At high fields $H > H_{c2}$ the ground state simply corresponds to a ferromagnetic alignment of spins. In the model with only nearest-neighbor exchange J the four spin-wave modes (according to a number of ions in a unit cell) are given as

$$\nu_{1,2} = \tilde{\gamma}H - 8JS, \quad \nu_{3,4} = \tilde{\gamma}H - 2JS(2 \mp \sqrt{1 + 3\eta_k}), \quad (4)$$

where η_k is a certain combination of lattice harmonics ($\eta_{k=0}=1$).¹¹ The first two branches are soft modes with no dispersion in the nearest-neighbor exchange approximation, acquiring a finite gap above the saturation field $\tilde{\gamma}H_{c2}=8JS$. Additional interactions produce the weak dispersion, result-

ing in a finite gaps at $\mathbf{k}=0$. We suggest that lines E and $E1-E2$ of the spectrum demonstrating exact linear field dependences with small gaps at $H=H_{c2}$ ($\nu_{1,2}(H_{c2})=6$ GHz for $H\parallel[111]$ and 7 and 15 GHz for $H\perp[111]$) correspond to this type of modes. The other two modes are dispersive magnon branches with gaps $\nu_{3,\mathbf{k}=0}=0$ and $\nu_{4,\mathbf{k}=0}=\tilde{\gamma}H_{c2}$. Line D in Figs. 2–4 should be ascribed to the mode ν_3 while the last mode ν_4 lies in a frequency range of about 200 GHz, unreachable in the present experimental conditions. At intermediate fields $H_{c1}<H<H_{c2}$ we have observed one intensive resonance mode (line C) which appears above H_{c1} and softens towards H_{c2} , pointing at a continuous second-order nature of this transition. Should there exist a self-consistent microscopic theory giving the correct ground state of the system, the values of $\nu_{1,2}(H_{c2})$ as well as the field evolutions of the $\nu_{3,\mathbf{k}=0}$ and line C can be useful to determine the spin-Hamiltonian constants.

In conclusion, a detailed study of the magnetic resonance in a pyrochlore antiferromagnet $\text{Gd}_2\text{Ti}_2\text{O}_7$ was carried out. In the disordered state the system demonstrates a paramagnetic resonance absorption gradually converting into nonresonant

absorption in the vicinity of the ordering transition. Below the transition, a clear antiferromagnetic resonance spectrum was observed. Its low-field part is qualitatively described in the hydrodynamic approximation applied to the nonplanar magnetic ordering with cubic or tetrahedral symmetry which is consistent with the recently proposed $4k$ structure. In the spin-saturated phase, our experiment provides direct observation of the quasilocal soft modes in a pyrochlore magnet. We also succeeded in tracing their fields evolution in magnetic fields above saturation which confirms the theoretical predictions and previous observations of the magnetocaloric effect.

ACKNOWLEDGMENTS

The authors thank V.I. Marchenko, O.A. Petrenko, and V.N. Glazkov for valuable discussions. This work was in part supported by INTAS YSF 2004-83-3053, the Russian Fund for Basic Research, Grant No. 04-02-17294, and the RF President Program. S.S.S. is also grateful to the National Science Support Foundation.

¹J. Villain, *Z. Phys. B* **33**, 31 (1979).

²A. P. Ramirez *et al.*, *Phys. Rev. Lett.* **89**, 067202 (2002).

³O. A. Petrenko, M. R. Lees, G. Balakrishnan, and D. McK. Paul, *Phys. Rev. B* **70**, 012402 (2004).

⁴P. Bonville, J. A. Hodges, M. Ocio, J.-P. Sanchez, P. Vulliet, S. Sosin, and D. Braithwaite, *J. Phys.: Condens. Matter* **15**, 7777 (2003).

⁵J. R. Stewart, G. Ehlers, A. S. Wills, S. T. Bramwell, and J. S. Gardner, *J. Phys.: Condens. Matter* **16**, L321 (2004).

⁶N. P. Raju, M. Dion, M. J. P. Gingras, T. E. Mason, and J. E. Greedan, *Phys. Rev. B* **59**, 14489 (1999).

⁷O. Cépas, A. P. Young, and B. S. Shastry, *Phys. Rev. B* **72**, 184408 (2005).

⁸A. S. Wills, M. E. Zhitomirsky, B. Canals, J.-P. Sanchez, P. Bonville, P. Dalmas de Reotier, and A. Yaouanc, *J. Phys.: Condens. Matter* **18**, L37 (2006).

⁹S. E. Palmer and J. T. Chalker, *Phys. Rev. B* **62**, 488 (2000).

¹⁰S.-H. Lee, C. Broholm, W. Ratcliff, G. Gasparovic, Q. Huang, T. H. Kim, and S.-W. Cheong, *Nature (London)* **418**, 856 (2002).

¹¹M. E. Zhitomirsky, *Phys. Rev. B* **67**, 104421 (2003).

¹²S. S. Sosin *et al.*, *Phys. Rev. B* **71**, 094413 (2005).

¹³G. Balakrishnan, O. A. Petrenko, M. R. Lees, and D. McK. Paul, *J. Phys.: Condens. Matter* **10**, L723 (1998).

¹⁴A. K. Hassan, L. P. Levy, C. Darie, and P. Strobel, *Phys. Rev. B* **67**, 214432 (2003).

¹⁵A. F. Andreev and V. I. Marchenko, *Sov. Phys. Usp.* **23**, 21 (1980).

¹⁶V. N. Glazkov *et al.*, *Phys. Rev. B* **72**, 020409(R) (2005).

¹⁷L. D. Landau and E. M. Lifshits, *Quantum Mechanics* (Pergamon, Oxford, 1980).

¹⁸Y. Narumi (private communication).

¹⁹A. Yaouanc *et al.*, *Phys. Rev. Lett.* **95**, 047203 (2005).